Ann. Phys. (Leipzig) **15**, No. 7 – 8, 596 – 605 (2006) / **DOI** 10.1002/andp.200510202

# Superconducting fluctuations in $Bi_2Sr_2Ca_{1-x}Dy_xCu_2O_{8+\delta}$ as seen by terahertz spectroscopy

**J. Orenstein**[1,*], **J. Corson**[1,**], **Seongshik Oh** [2,***], and **J. N. Eckstein**[2]

[1] Physics Department, University of California, Berkeley and
Materials Science Division, Lawrence Berkeley National Laboratory, Berkeley, CA 94720, USA
[2] Department of Physics, University of Illinois, Urbana, Illinois 61801, USA

Received 15 November 2005, revised 2 February 2006, accepted 6 February 2006
Published online 26 May 2006

**Key words** High-temperature superconductors, vortex plasma, superconducting fluctuations, time-domain THz spectroscopy.

**PACS** 74.25.Gz, 78.47.+p

*In commemoration of Paul Drude (1863–1906)*

More than one hundred years ago Paul Drude derived the frequency-dependent conductivity $\sigma(\omega)$ of a gas of point charges, showing that the width of the spectrum was related to the scattering rate of carriers. Seventy five years later, in the late 1970's and early 1980's, it was recognized that $\sigma(\omega)$ of a two-dimensional superconductor above it's transition temperature $T_c$ could be described by the Drude response of interpenetrating gases of electrons and vortices. Here we describe measurements of $\sigma(\omega)$ in the high-$T_c$ superconductor system $Bi_2Sr_2Ca_{1-x}Dy_xCu_2O_{8+\delta}$ (BSCCO) using time-domain THz spectroscopy that provide evidence for vortices above $T_c$. We compare this evidence with results obtained by other probes of fluctuations in cuprate superconductors.



## 1 Introduction

The defining characteristic of a superconductor is the breaking of gauge symmetry and the establishment of long-range phase order. The phase order is maintained by the appearance of a phase stiffness, a measure of the energy cost of fluctuations from spatial uniformity. The free energy of such fluctuations is proportional to $\int d^D r \rho_s \nabla^2 \phi$ where $\rho_s$ is the stiffness of the phase, $\phi$, of the superconducting order parameter. A unique aspect of two dimensions ($D = 2$) is that $\rho_s$ has the units of energy. We will see that the ratio of $\rho_s$ to the temperature $T$ plays a crucial role in the theory of $\sigma(\omega)$ of the superconductor.

If phase rigidity defines the superconducting state, its destruction as $T$ is raised through $T_c$ must reflect the loss of phase order. The Kosterlitz-Thouless-Berezinski (KTB) [1–3] theory of melting in 2D demonstrated that the restoration of symmetry at $T_c$ takes place via the thermal generation of free vortices. Below $T_c$, vortices exist as bound pairs of opposite vorticity. The loss of long-range phase order at $T_c$ occurs when the first pair of vortices unbinds. Perhaps the most celebrated prediction of the theory is that these first free vortices appear when $T$ reaches the KTB transition temperature $T_{KT} \equiv \pi\rho_s/8$, at which point $\rho_s$ drops discontinuously to zero [4].

The KTB theory implies that the "normal" state above $T_c$ is in reality a vortex plasma (VP), a gas of bound and free vortices. However, the VP state can be difficult to observe in conventional, relatively

* Corresponding author E-mail: joeo@mh1.lbl.gov
** Present address: Agilent Laboratories, Palo Alto, CA 93406, USA
*** Present address: National Institute of Standards and Technology, 325 Broadway, Boulder, CO 80305, USA

clean BCS superconductors. Vortices exist in the normal state only when the order parameter amplitude is well-defined, that is, in the interval between $T_c$ and the mean-field transition temperature $T_{MF}$ (the $T$ to which superconductivity would persist if phase fluctuations could be suppressed). In clean-limit 2D superconductors, where the zero-$T$ phase stiffness $\rho_s(0)$ is essentially the Fermi energy, the VP exists only in a narrow range $T_{MF} - T_c \sim T_c^2/E_F$.

The high-$T_c$ cuprate superconductors are in the clean-limit and thus one might naively expect a very limited VP regime. However, two aspects of these materials suggest the possibility of a larger range of phase fluctuations [5]. The first is strong electron-electron correlations, which cause $\rho_s(0)$ to vanish as $x$, the deviation from one-electron per site, goes to zero. If the pairing amplitude remains nonzero in the same limit, then we would expect a VP regime whose size relative to $T_c$ would grow as $x \to 0$. The second factor is spatial inhomogeneity, which has been observed in the cuprates on a variety of time and length scales. The simplest example is static inhomogeneity in the local value of $T_{MF}$, such as obtained in a granular superconductor. Here the size of the phase fluctuation regime can be arbitrarily large, extending from the largest local values of $T_{MF}$ to the smallest.

Quantifying the extent of the VP state in $T$ and $x$ can play a major role in unravelling the physics of the cuprates, where a central question is the origin of the crossovers above $T_c$ seen by different probes. For example, if $T_{MF}(x)$ can be determined, then a comparison with the pseudogap onset temperature, $T^*(x)$, will address the long-standing question of the relationship between superconducting pairing and the correlations that give rise to the pseudogap. In addition, characterizing $T_{MF}(x)$ in cuprate systems known to possess different degrees of spatial inhomogeneity helps to define where granularity (in its most general sense) plays a role in determining $T_c$.

As is the case with most issues in the cuprates, determining the boundaries of VP state has not proved to be straightforward. Recently, evidence for a VP regime above $T_c$ has been obtained from terahertz (THz) conductivity [6], Nernst effect [7–13], and magnetic susceptibility measurements [14, 15]. However, the different probes appear to yield different crossover temperatures. The question we address in this paper is the interpretation of the THz conductivity and its relationship to other probes of superconducting fluctuations. In the next section we review theoretical predictions for ac conductivity in the VP state. In Sect. 3 we compare these predictions with experimental results. In Sect. 4 we conclude with a discussion of the ac conductivity in the context of other probes of superconducting fluctuations in the normal state.

## 2 Ac conductivity in the vortex plasma regime

The condensate contribution to the ac conductivity of a 2D superconductor above $T_c$ obeys the scaling relation,

$$\frac{\sigma(\omega)}{\sigma_0} = \frac{\Omega_0}{\Omega} S(\omega/\Omega), \tag{1}$$

where $\Omega$ is the inverse of the order parameter correlation time and $\sigma_0$ is the conductivity as $\Omega$ approaches its bare value $\Omega_0$ [16]. (To obtain the total conductivity we must add the Drude contribution from the normal state quasiparticles). The ac conductivity of a VP is a specific case of this general relation. Many of the properties of the VP conductivity can be obtained by considering the limits of high and low frequency. In the $\omega/\Omega \to \infty$ limit, vortices are static on the scale of the time-variation of the applied current and the conductivity approaches that of a superconductor, that is $\sigma(\omega) \to \sigma_Q \rho_{s0}/(-i\omega)$, where $\sigma_Q \equiv e^2/\hbar d$ and $d$ is the bilayer thickness. This requires that $S(\omega/\Omega) \to \Omega/(-i\omega)$ and identifies $\sigma_0\Omega_0$ as $\sigma_Q\rho_{s0}$. Here $\rho_{s0}$ is the "bare" superfluid density, as distinguished from the "renormalized" superfluid density $\rho_s$. The existence of a superfluid response at high frequency, i.e., $\rho_{s0} > 0$, in a regime where $\rho_s = 0$, is the defining characteristic of the VP state. In the opposite, $\omega/\Omega \to 0$ limit, the vortices move in response to the current, and the conductivity is the inverse of the flux-flow resistivity, $\rho_{ff} = (n_F\phi_0^2 D/T)$, where $n_F$ is the density of free vortices, $\phi_0$ is the flux quantum, and $D$ is the vortex diffusivity. Combining the two limits, we can

infer that $\Omega = \pi^2(\rho_{s0}/T)Dn_F$, indicating that $\Omega$ is essentially the inverse time required for vortices to diffuse the average distance between them. We can also express $\Omega$ in the form $(\Omega/\Omega_0) = n_F A_c$, where $A_c$ is the area of the vortex core and $\Omega_0^{-1} \equiv [\pi^2(\rho_{s0}/T)(D/A_c)]^{-1}$ is roughly the time for a vortex to diffuse a core radius. The dimensionless factor $n_F A_c$ is the probability that a site that can accommodate a vortex is occupied. Finally, we note that as $\sigma_0\Omega_0 = \sigma_Q\rho_{s0}$, the scaling relation can be rewritten in the form [17–19],

$$\frac{\sigma(\omega)}{\sigma_Q} = \frac{\rho_{s0}}{\Omega} S(\omega/\Omega). \tag{2}$$

As Eq. (2) indicates, the behavior of $\sigma(\omega, T)$ in the VP state is largely determined by $\Omega(T)$. The features of $\sigma(\omega, T)$ that identify a KTB transition follow from the essential singularity in $\Omega(T)$ that is predicted to occur at $T_{KT}$. In view of the importance of $\Omega(T)$ in identifying and characterizing the transition to the VP state, below we briefly describe a heuristic derivation of this quantity, following a discussion by Minnhagen [18].

As we have seen, $\Omega(T)$ depends linearly on the free vortex density, $n_F$. On the other hand, $n_F$ itself depends upon $\Omega(T)$ because the latter is connected to the intervortex screening length $\xi(T)$, through the relation, $\xi^2 = D/\Omega$, or equivalently, $\xi^2 = \pi^2 n_F \rho_{s0}/T$. These relationships lead to a self-consistency condition that ultimately determines $\Omega(T)$. Specifically, we note that $n_F$ is given by a Boltzmann factor, $n_F A_c = \exp(-E_V/T)$, where $E_V$ is free vortex creation energy. $E_V$ is the sum of the core energy $E_c$ and one-half the energy required to separate a vortex-anti-vortex pair to infinity. Because the logarithmic inter-vortex interaction is cutoff at $\xi$, we have that $E_V = E_c + (\pi\rho_{s0}/4)ln(\xi/\xi_0)$, where $\xi_0 \sim A_c^{1/2}$. Satisfying the two conditions imposed on $n_F$ leads to the $T$ dependence of the phase fluctuation rate,

$$\frac{\Omega}{\Omega_0} = \left(e^{-E_c/T}\right)^{\frac{T}{T-\pi\rho_s/8}}. \tag{3}$$

From Eq. (3) we see that $\Omega(T)$ goes to zero very rapidly as $T$ approaches $T_{KT} \equiv \pi\rho_s/8$.

Although all VP's obey Eq. (2), all VP's are not the same. The "fingerprints" of a specific VP state are the microscopic length and frequency scales, $\xi_0$ and $\Omega_0$, the bare phase stiffness, $\rho_{s0}(T)$, and the vortex core energy $E_c(T)$. Any information regarding the physics that underlies a given VP state must come from these parameters, as once they are specified the phase correlation time $\Omega(T)$ and length $\xi(T)$ are determined by universal VP relations.

Historically, interest in the phase fluctuations of 2D superconductors has focused on $T$'s very near to $T_c$, where the predictions of a universal jump $\rho_s$ and the essential singularity in $\Omega(T)$ (or the corresponding length scale $\xi(T)$) can be tested. However, the main interest in the context of the high-$T_c$ cuprate superconductors is entirely different. It is clear that near $T_c$ the transition cannot be of the KTB type because of the nonzero (and in some compounds, strong) interlayer coupling. The focus shifts to the possibility of a VP state arising when the layers decouple above $T_c$, and especially to the question of how high in $T$ it might persist.

## 3 Terahertz conductivity results

### 3.1 $\sigma(\omega, T)$ of an underdoped ($T_c$=71 K) sample

In principle, $\sigma(\omega)$ measured over any range of frequency can directly probe the persistence of $\rho_{s0}$ above $T_c$. However, in practice, $\sigma(\omega)$ rapidly becomes too small to be measured when $\omega/\Omega \ll 1$. Thus sensitivity to $\rho_{s0}(T)$ is lost well below $T_{MF}$ if the measurement frequency range lies much below $\Omega_0$. We can estimate $\Omega_0$ from the Bardeen-Stephen [20] assertion that $\rho_{ff}$ extrapolates linearly to the normal resistivity, $\rho_n$, as $n_F A_c \to 1$, which leads to $D/A_c = \overline{\rho}_n T/\pi^2$ and $\Omega_0 = \overline{\rho}_n \rho_s$, where $\overline{\rho}_n \equiv \rho_n \sigma_Q$. Evaluating $\Omega_0$ for parameters appropriate to the cuprates yields $\Omega_0 \sim$ 1-10 THz. Thus, in order to probe the full extent to which $\rho_{s0}$ survives in the normal state it is necessary to probe the conductivity on the THz frequency scale.

We have measured $\sigma(\omega)$ in a set of underdoped $Bi_2Sr_2Ca_{1-x}Dy_xCu_2O_{8+\delta}$ (BSCCO) samples using the technique of time-domain transmission spectroscopy in the range from 0.1-0.6 THz [6]. Direct measurement

 

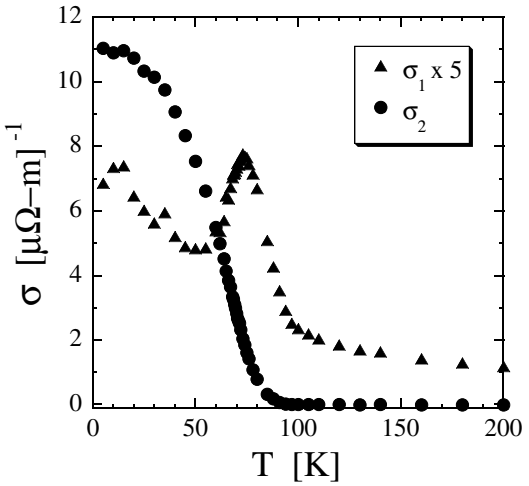


**Fig. 1** The complex conductivity $\sigma$ measured at 100 GHz, as a function of the temperature $T$. The real part, $\sigma_1$, is multiplied by 5 for ease of comparison with the imaginary part $\sigma_2$.

of electric fields rather than power yielded both the real and imaginary parts of $\sigma(\omega)$, which is crucial for the scaling analysis. The samples were thin ($\sim 50$ nm) films grown by atomic layer-by-layer epitaxy. Fig. 1 shows the real and imaginary parts of the conductivity, $\sigma_1$ and $\sigma_2$, at 100 GHz for an underdoped BSCCO film with $T_c$=71 K. The dissipative component, $\sigma_1$, has a peak centered near $T_c$ superposed on a rising background, while $\sigma_2$ becomes observable near 100 K.

The quantity best suited to show the persistence of $\rho_{s0}$ into the normal state is $T_\Theta(\omega) \equiv \omega\sigma_2(\omega, T)/\sigma_Q$, which approaches $\rho_{s0}(T)$ when $\omega \gg \Omega$. Fig. 2 shows $T_\Theta(\omega)$ as a function of $T$ on a semilog scale for the sample shown in Fig. 1 and for our most underdoped sample with $T_c$=33 K. This plot identifies a crossover in the dynamics with increasing temperature. At low $T$, $T_\Theta$ is frequency independent. As $T$ increases, $T_\Theta$ fans out, with lowest frequency data decreasing most rapidly. All samples that we have measured show the behavior described above. Furthermore, we find that for all samples the value of $T_\Theta$ at the crossover, and the $T$ at which it occurs, are related linearly. The dashed line in Fig. 2 shows that the crossover is described by the simple relation, $T_\Theta = (8/\pi)T$.

The appearance of a crossover at the KT temperature suggests that we analyze $\sigma(\omega)$ further using the scaling relation (Eq. (2)). By comparing $\sigma(\omega)$ to Eq. (2), we can extract both $\rho_{s0}(T)$ and $\Omega(T)$. As the first step, we note that the phase of the complex conductivity, $\phi \equiv \tan^{-1}(\sigma_2/\sigma_1)$, equals the phase of

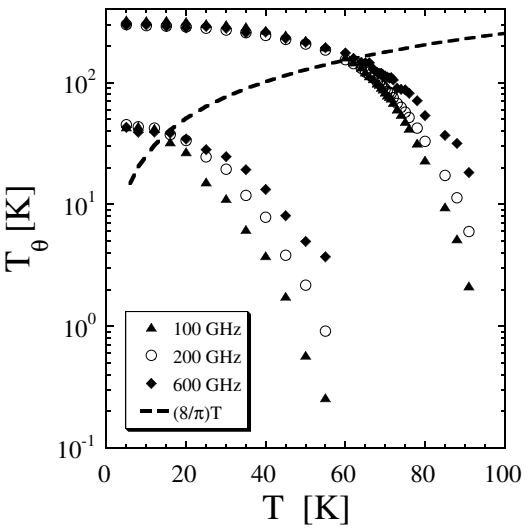


**Fig. 2** The dynamic (frequency dependent) phase-stiffness temperature, $T_\Theta(\omega) \equiv \omega\sigma_2(\omega)/\sigma_Q$ as a function of temperature $T$. Data are shown for two samples, one with $T_c$=33 K (left side) and the other with $T_c$=71 K (right side). The dashed line corresponds to the KTB condition for 2D melting, i.e., phase stiffness and temperature related by $T_\Theta = (8/\pi)T$.

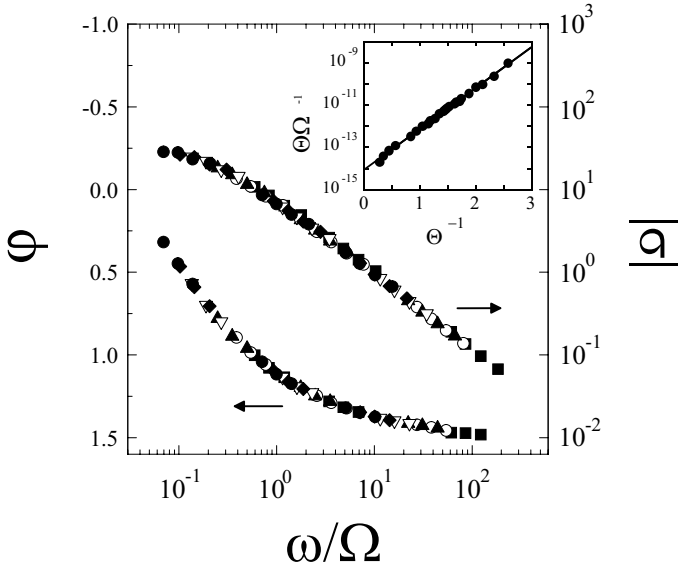


**Fig. 3** Conductivity phase angle, $\phi = \tan^{-1}(\sigma_2/\sigma_1)$, and normalized conductivity magnitude $|\sigma|$, plotted as a function of the reduced frequency $\omega/\Omega(T)$. Each plot comprises measurements with $T$ in the range from 64 to 91 K, and frequency from 100 to 400 GHz.

$S(\omega/\Omega)$, and therefore depends only on $\Omega$. In determining $\phi$ we include only the fluctuation contribution to $\sigma_1$, which is obtained by subtracting the broad quasiparticle background from the peak seen in Fig. 1. With the appropriate choice of $\Omega(T)$, $\phi(T)$ should collapse to a single curve when plotted as a function of the normalized frequency $\omega/\Omega$. Once $\Omega(T)$ is known, $\rho_{s0}(T)$ is obtained from a collapse of the normalized conductivity magnitude, $(\hbar\Omega/\rho_{s0})|\sigma(\omega)|/\sigma_Q$ to $|S(\omega/\Omega)|$. Fig. 3 shows the collapse of the data to the phase and magnitude of $S$. As anticipated, $S$ approaches a real constant in the limit $\omega/\Omega \to 0$, and approaches $i\Omega/\omega$ as $\omega/\Omega \to \infty$.

In Fig. 4 we present the behavior of the bare stiffness and phase-correlation time obtained from the scaling analysis of $\sigma(\omega)$. The main panel contrasts $\rho_{s0}(T)$ (referred to as $T^0_\Theta$ in the legend) with the dynamical phase stiffness $T_\Theta(\omega)$ measured at 150 and 400 GHz. The inset shows $\tau \equiv \Omega^{-1}$ as a function of temperature together with hashes that highlight the region where $\tau < \hbar/k_BT$.

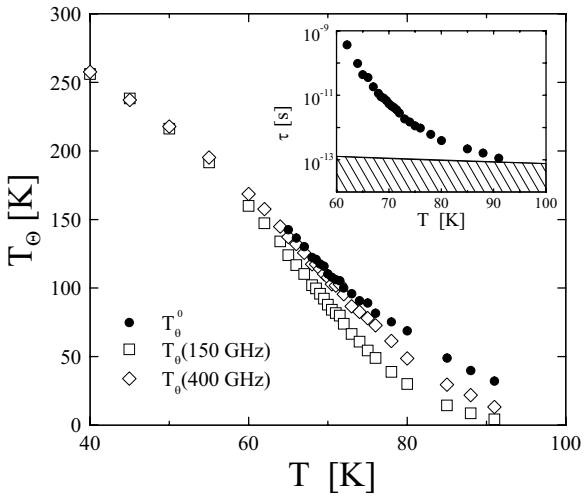


**Fig. 4** The bare phase-stiffness $\rho_{s0}$ and phase correlation time $\tau \equiv \Omega^{-1}$ found from the scaling analysis of $\sigma(\omega, T)$, plotted as a function of $T$. *Main panel:* Comparison of $\rho_{s0}$, shown as solid circles, with $T_\Theta(\omega)$ at 150 GHz (open squares) and at 400 GHz (open diamonds). *Inset:* $\tau$ on a semi-log plot. The hash marks define a region where $\tau$ is less than the lifetime of electrons in the normal state, $\hbar/k_BT$.

 

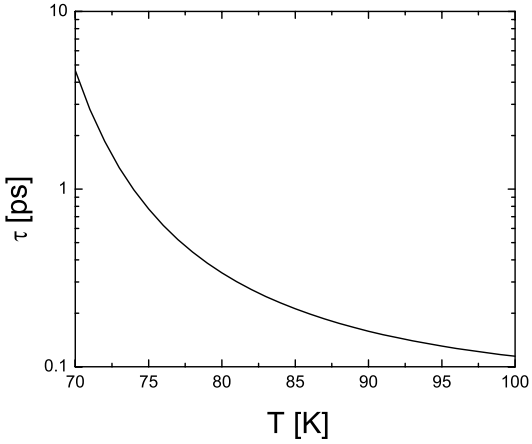


**Fig. 5** Phase correlation time $\tau(T)$ as calculated from Eq. (3), with parameters as given in text.

The parameters displayed in Fig. 4 suggest that while phase correlations indeed persist above $T_c$, their effect on conductivity vanishes well below $T^*$. Near 95 K (in this sample), $\tau$ falls to $\hbar/k_BT$, which is approximately the normal quasiparticle lifetime. Above this $T$, any contribution to $\sigma(\omega)$ from superconducting fluctuations becomes indistinguishable from the response of the normal electrons.

### 3.2 Comparison with VP predictions

In this section we compare the THz measurements on the $T_c$=71 K sample with the VP predictions, beginning with $\tau(T)$ as obtained by scaling analysis of $\sigma(\omega)$. According to Eq. (3), $\tau(T)$ depends on $\rho_{s0}(T)$, $\tau_0 \equiv \Omega_0^{-1}$, and $E_c$. Fig. 5 shows a plot of $\tau$ calculated according to Eq. (3) based on $\rho_{s0}(T)$ shown in Fig. 4, with $E_c = 0.3\rho_{s0}$ and $\tau_0 = 0.14$ picoseconds. The theoretical curve captures the main features of the data. The value of $\tau_0$ is in reasonable agreement with the prediction $(\overline{\rho}_n\rho_{s0})^{-1}$, which is 0.4 picoseconds for this sample. The coefficient 0.3 can be compared with the Ginzburg-Landau prediction that $E_c = 0.6\rho_{s0}$ [21]. The vortices can be considered to be "cheap" [22–24] as the core energy is on the scale of $\rho_{s0}$, rather than $E_F$. The question of whether they are "fast" [25] as well, that is the relation of $D$ to Bardeen-Stephen prediction, will be addressed when we compare the THz conductivity and magnetic susceptibility, $\chi$.

We turn next to the VP prediction for $\sigma(\omega, T)$, which requires knowledge of the scaling function, $S(\omega\tau)$, in addition to $\rho_{s0}(T)$ and $\tau(T)$. Minnhagen [18] has suggested a simple form, $S_2(\omega\tau) = 1/(1+\omega\tau)$, that is consistent with many computer simulations and experiments on model KTB systems. In Fig. 6 we show the prediction for $\omega\sigma_2(T)/\sigma_Q$ based the Minnhagen scaling function, for several values of $\omega$ that are close

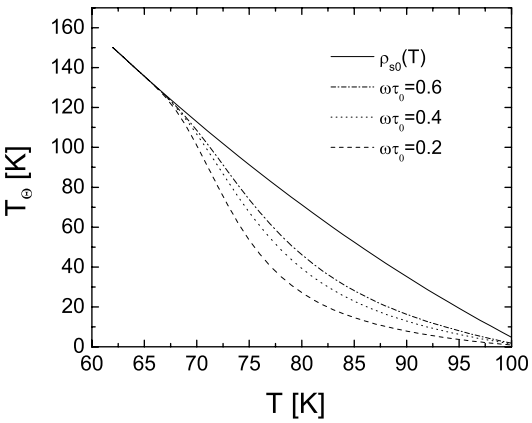


**Fig. 6** Dynamic superfluid density, $\omega\sigma_2/\sigma_Q$, calculated according to the Minnhagen scaling function described in the text, using $\rho_s(T)$ shown as solid line and $\tau$ as shown in Fig. 5 as input parameters.

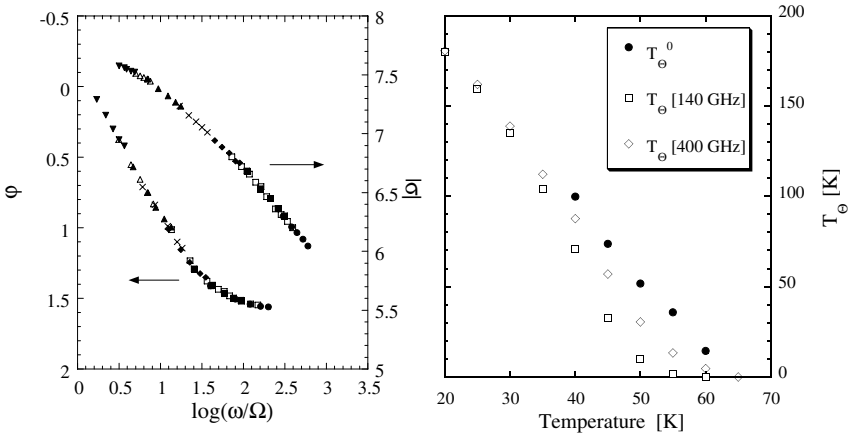


**Fig. 7** *Left panel:* conductivity phase and normalized magnitude as a function of scaled frequency for the 51 K underdoped sample. *Right panel:* bare phase stiffness, $\rho_s$, and dynamic phase stiffness, $T_\Theta(\omega)$, obtained from the scaling analysis.

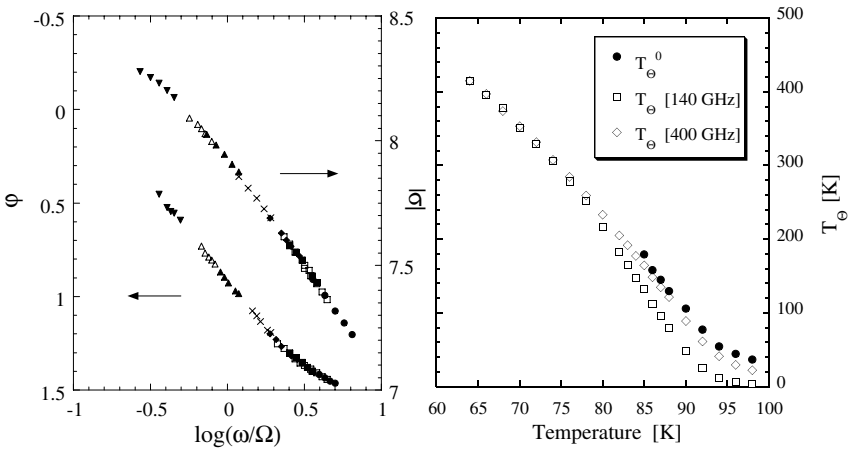


**Fig. 8** *Left panel:* conductivity phase and normalized magnitude as a function of scaled frequency for the 85 K underdoped sample. *Right panel:* bare phase stiffness, $\rho_s$, and dynamic phase stiffness, $T_\Theta(\omega)$, obtained from the scaling analysis.

to $1/\tau_0$. The strong singularity of $\tau(T)$ causes all the curves to fan out near $T_{KT}$, in reasonable agreement with the THz measurements.

### 3.3 THz conductivity in samples with different hole concentration

To investigate how $\rho_{s0}(T)$ and $\tau(T)$ depend on hole concentration, we analyzed the THz conductivity of two additional underdoped BSCCO films, with $T_c$'s of 51 K and 85 K. The scaling analysis and $\rho_{s0}(T)$ are shown in Figs. 7 and 8. In Fig. 9, we show $\tau(T)$ for the three samples that were analyzed. The $\rho_{s0}(T)$ and $\tau(T)$ of the samples with $T_c$'s of 51 K and 85 K show the same features as the $T_c$=71 K sample considered previously. The phase fluctuation rate reaches $k_BT/\hbar$ at a $T$ that is within 10-20 K above $T_c$ and is well below the pseudogap temperature $T^*$. The superfluid density decays approximately linearly with $T$ and extrapolates to zero at roughly the same $T$ at which the phase fluctuation rate reaches $k_BT/\hbar$.

 

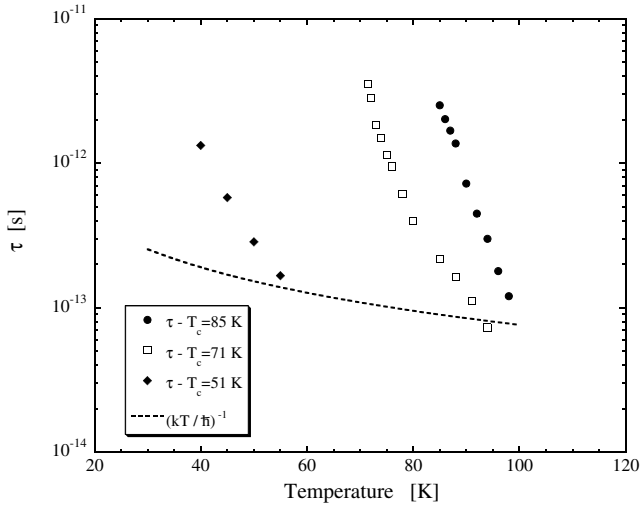


**Fig. 9** The lifetime of phase fluctuations for the 51K, 71K, and 85K underdoped samples. The dashed line illustrates the mean-free-time of normal state quasiparticles, which is $\sim \hbar/k_B T$. For each of the samples the highest $T$ point plotted marks the $T$ at which fluctuation conductivity is no longer observed.

## 4 Comparison with other probes of superconducting fluctuations

Ong, Wang, and collaborators have explored superconducting fluctuations in a large number of cuprates through detailed measurements of the Nernst effect [7–13], and magnetization [14, 15]. As the theoretical understanding of the fluctuation diamagnetism is more advanced, we first compare $\sigma(\omega, T)$ and the magnetic susceptibility, $\chi(T)$. The latter quantity is directly related to $\rho_{s0}(T)$ and the phase correlation length, that is, $\chi \sim \rho_{s0}\xi^2$. The dynamic conductivity evaluated at the phase fluctuation frequency, $\sigma_1(\Omega, T)$ is $\sim \rho_{s0}\tau$. Thus $\chi(T)$ and $\sigma_1(\Omega, T)$ are both proportional to $\rho_{s0}$, with the former linked to the diverging length scale and the latter to the diverging time scale. In VP models, they are related through the vortex diffusivity,

$$D^{-1} = \frac{\mu_0}{8\pi}\frac{\sigma(\Omega, T)}{\chi(T)} = \frac{\mu_0}{4\pi}\frac{\sigma_1(0, T)}{\chi(T)}, \tag{4}$$

a formula that has the form of an Einstein relation for the VP.

To test the prediction of Eq. (4), it would be highly desirable to measure $\chi(T)$ and $\sigma(\omega, T)$ in the same samples. While this has not been done as yet, Li et al. [15] have measured $\chi(T)$ in an underdoped BSCCO crystal with a $T_c$ of 86 K, which is quite close to that of one of the samples whose THz conductivity we have analyzed. From the ratio of $\chi(T)$ (as shown in Fig. 4 of [15]) to $\sigma(\omega, T)$ (for the the BSCCO film with $T_c$=85 K), we estimate from Eq. (4) that $D \sim 0.001$-$0.01$ m$^2$/s. The VP picture of the fluctuating state suggests that we compare this result with the Bardeen-Stephen prediction that $D/A_c = T\overline{\rho}_n/\pi^2$. For the Bardeen-Stephen $D$ to coincide with the value obtained from the Einstein relation, we must have $A_c \sim 6\times10^{-15}$ m$^2$, corresponding to a core size of order $\sim 40$ nm. This is much larger than the core size of $\sim$ 2-3 nm that is seen in STM measurements or estimated from the Pippard length $v_F/\Delta$. Expressed slightly differently, if we were to substitute a core radius of order $v_F/\Delta$ into the Bardeen-Stephen formula we would obtain $D \sim 10^{-5}$ m$^2$/s, at least two orders of magnitude smaller than the what is needed to account for the observed $\chi/\sigma$. Thus the vortices would indeed have to be "big" [26] (compared with the scale set by $H_{c2}$) and therefore "fast" [25] to be consistent with the observed ratio of susceptibility to conductivity.

Interest in the VP state in the cuprates was greatly stimulated by extensive measurements of the Nernst effect by the Princeton group. The Nernst effect is the transverse voltage generated by a thermal gradient in the presence of a magnetic field perpendicular to the conducting plane. Because of the transverse geometry the Nernst effect plays same role for vortex transport as thermopower for quasiparticle transport. While at present a detailed theoretical understanding of the effect is lacking, it is clear from measurements below $T_c$ that it is highly sensitive to the presence of a vortex plasma (or liquid) state. The more subtle issue is the inverse, i.e., when does a Nernst signal indicate the existence of a VP? As the VP regime crosses over

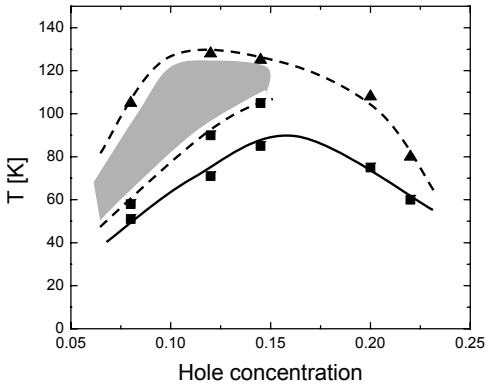


**Fig. 10** Comparison of onset temperatures of superconductivity, fluctuation conductivity, and Nernst effect in the BSCCO system. Nernst onset $T$'s (triangles) are from [14]. Shading illustrates the region in which the conductivity is essentially normal yet the Nernst signal is nonzero.

smoothly to a Gaussian fluctuation regime when the vortices become dense, we expect a smooth crossover in Nernst voltage as well. Thus it clear that merely the existence of a Nernst signal does not indicate a VP [27]. However, the Princeton group has shown that in a broad $T$ range above $T_c$ the Nernst signal is comparable to what is seen in the mixed state below $T_c$, strongly suggesting that a reasonably dilute VP persists in the normal state.

An especially interesting feature of the Nernst phenomenology is the disparity between the regime of VP sensed by the Nernst voltage and by conductivity measurements. We illustrate the trend in Fig. 10, which compares the onset temperatures of fluctuation conductivity $T_\sigma$ and Nernst signal, $T_N$. The $T_\sigma$'s, defined by the condition $\Omega(T_\sigma) = k_B T/\hbar$, are determined from Fig. 9, while the $T_N$'s are those quoted in [14]. It can be seen that the disparity in the onset $T's$ grows with decreasing $x$, and a large region of phase space appears with VP response seen in the Nernst effect, but not in conductivity. The contrast between $\sigma$ and the Nernst signal ($e_N$) seen when varying $T$ at $H = 0$ is mirrored by scans of $H$ at a fixed $T$ below $T_c$. In such measurements dc resistance and $e_N$ appear together, as the vortex lattice melts [14]. However, while $\rho_{dc}$ reaches $\rho_n$ quite rapidly, apparently representing the onset of the normal state, $e_N$ persists to a much higher $H$ [14].

Is it possible that the "Nernst region" can represent a relatively dilute VP, given that the phase fluctuation frequency has reached $\sim T$ at a far lower $T$? From our previous discussion we can write $\Omega \sim \rho_{s0}(D/T)n_F$, where $D/T$ is the vortex mobility. If Bardeen-Stephen dynamics are applicable, then the mobility is simply the vortex core area. In this case, when $\Omega \sim \rho_s \sim T$ the dimensionless vortex density $n_F A_c$ must be of order unity. Within the VP picture vortices can be dilute in such a regime only if $D/T \gg A_c$. Just as we concluded from the comparison of $\sigma$ and $\chi$, consistency of $\sigma$ and Nernst suggests that the vortices are "fast." Whether a fast vortex can emerge from either strong correlations or inhomogeneity in the cuprates is a fascinating area of future research.

**Acknowledgements** J. O. would like to acknowledge valuable discussions with Joel Moore, Ashwin Vishwanath, Yayu Wang, Andrew Millis, and Patrick Lee. This work was supported by NSF-9870258 and DOE-DE-AC03-76SF00098.

## References

[1] V. L. Berezinskii Sov. Phys. JETP **32**, 493 (1970).
[2] V. L. Berezinskii, Sov. Phys. JETP **34**, 610 (1972).
[3] J.M . Kosterlitz and D. J. Thouless, J. Phys. C **6**, 1181 (1973).
[4] J. M. Kosterlitz and D. R. Nelson, Phys. Rev. Lett. **39**, 1201 (1977).
[5] V. J. Emery and S. A. Kivelson, Nature **374**, 434 (1995).
[6] J. Corson et al., Nature **398**, 221 (1999).
[7] Z. A. Zu et al., Nature **406**, 486 (2000).
[8] Y. Wang et al., Phys. Rev. B **64**, 224519 (2001).

 

[9] Y. Wang et al., Phys. Rev. Lett. **88**, 257003 (2002).
[10] Y. Wang et al., Science **299**, 86 (2003).
[11] N. P. Ong and Y. Wang et al., Physica C **408**, 11 (2004).
[12] N. P. Ong et al., Ann. Phys. **13**, 9 (2004).
[13] Y. Wang et al., cond-mat/0503190.
[14] Y. Wang et al., cond-mat/0510470.
[15] L. Li et al., Europhys. Lett. in press cond-mat/050761.
[16] D. S. Fisher, M. P. A. Fisher, and D. A. Huse, Phys. Rev. B **43**, 130 (1991).
[17] B. I. Halperin and D. R. Nelson, J. Low Temp. Phys. **36**, 599 (1979).
[18] P. Minnhagen, Rev. Mod. Phys. **59**, 1001 (1987).
[19] P. Minnhagen and A. Jonsson, Phys. Rev. B **55**, 9035 (1997).
[20] J. Bardeen and M. J. Stephen, Phys. Rev. A **140**, 1197 (1965).
[21] C. R. Hu and R. S. Thompson, Phys. Rev. B **6**, 110 (1972).
[22] P. A. Lee, Physica C **388**, 7 (2003).
[23] C. Honerkamp and P. A. Lee, Phys. Rev. Lett. **92**, 177002 (2004).
[24] P. A. Lee, N. Nagaosa, and X.-G. Wen, Rev. Mod. Phys., in press, cond-mat/0410445.
[25] L. B. Ioffe and A. J. Millis, Phys. Rev. B **66**, 094513 (2002).
[26] P. A. Lee and X.-G. Wen, Phys. Rev. Lett. **78**, 4111 (1997).
[27] I. Ussishkin, S. L. Sondhi, and D. A. Huse, Phys. Rev. Lett. **89**, 287001 (2002).